Hydrol. Earth Syst. Sci., 17, 103–118, 2013
www.hydrol-earth-syst-sci.net/17/103/2013/
doi:10.5194/hess-17-103-2013

Hydrology and Earth System Sciences

Macropore flow of old water revisited: experimental insights from a tile-drained hillslope

J. Klaus[1], **E. Zehe**[2], **M. Elsner**[3], **C. Külls**[4], **and J. J. McDonnell**[1,5]

[1]Global Institute for Water Security, University of Saskatchewan, Saskatoon, SK, Canada
[2]Chair of Hydrology, Institute for Water Resources and River Basin Management, Karlsruher Institute of Technology KIT, Karlsruhe, Germany
[3]Helmholtz Center Munich, Munich, Germany
[4]Institute of Hydrology, Albert-Ludwigs-Universität Freiburg, Freiburg, Germany
[5]University of Aberdeen, School of Geoscience, Aberdeen, UK

Correspondence to: J. Klaus (julian.klaus@usask.ca)

Received: 22 March 2012 – Published in Hydrol. Earth Syst. Sci. Discuss.: 2 April 2012
Revised: 30 November 2012 – Accepted: 4 December 2012 – Published: 16 January 2013

Abstract. The mechanisms allowing the rapid release of stored water to streams are poorly understood. Here we use a tile-drained field site to combine macroporous soils at the hillslope scale with the advantage of at least partly controlled lower boundary conditions. We performed a series of three irrigation experiments combining hydrometric measurements with stable isotope and bromide tracers to better understand macropore–matrix interactions and stored water release processes at the hillslope scale. Stable isotope concentrations were monitored in the irrigation water, the tile-drain discharge and the soil water before and after the experiment. Bromide was measured every 5–15 min in the tile-drain hydrograph. Different initial conditions for each experiment were used to examine how these influenced flow and transport. Different amounts of irrigation water were necessary to increase tile-drain discharge above the baseflow level. Hydrograph separation based on bromide data revealed that irrigation water contributions to peak tile-drain discharge were on the order of 20 %. Oxygen-18 and deuterium data were consistent with the bromide data and showed that pre-event soil water contributed significantly to the tile-drain event flow. However, the isotopic composition of soil water converged towards the isotopic composition of irrigation water through the course of the experiment. Mixing calculations revealed that by the end of the irrigation experiments 20 % of the soil water in the entire profile was irrigation water. The isotopic data showed that the pre-event water in the tile drain was mobilized in 20–40 cm soil depth where the macropore–matrix interaction leads to an initiation of macropore flow after a moisture threshold is exceeded.

1 Introduction

Macropore flow of old water has been observed for over 20 yr now (McDonnell, 1990) but there is still much ongoing discussion regarding whether this rapid effusion of old, pre-event water, is indeed preferential flow or pressure wave displacement (Torres et al., 1998; Williams et al., 2002) or some combination of both. These questions lie at the heart of the double paradox, as outlined by Kirchner (2003) and tested by Bishop et al. (2004), and quantification of flow and transport processes that connect the plot, hillslope and catchment scales. Studies generally have shown that preferential flow can have a strong influence on runoff processes at the hillslope (Mosley, 1979; Tsukamoto and Ohta, 1988; Smettem et al., 1991; Tsuboyama et al., 1994; Noguchi et al., 1999; Uchida et al., 1999) and the catchment scale (Sidle et al., 2000; Blöschl and Zehe, 2005; Zehe et al., 2007) with important controls on contaminant transport (e.g. Sidle et al., 1977; Flury et al., 1995; Šimůnek et al., 2003). Other studies have shown that preferential flow itself can be a direct reflection of new water and dissolved substances that bypass the soil matrix and move to depth within the soil profile (Jarvis,

2007). The amount of preferential flow is often equated to the amount of "new" water (Stone and Wilson, 2006). Beyond the issue of preferential flow versus pressure wave release and effusion of pre-event water is the dual question of where and how mixing occurs on the event timescale: that is, where and how the event water loses its "newness". The hillslope scale is a key, as this represents the scale at which plot-scale processes (often very precisely defined in laboratory and column experiments) combine to yield a signature that ultimately becomes streamflow. This is a difficult problem due to the blackbox nature of subsurface mixing and, perhaps as importantly, the lack of any boundary control on quantifying such processes.

Several studies have shown that flow and transport at the hillslope scale are a combination of some matrix flow/displacement processes mixed with preferential flow. The ratios of matrix flow versus preferential flow vary widely. For instance, Leaney et al. (1993) found that at the plot scale, sampled subsurface stormflow consisted mainly of storm rainfall ($> 90\,\%$) that was transported via macropores bypassing the soil matrix. Vogel et al. (2008) performed a modeling study using a dual continuum approach combined with sampled oxygen-18 (^{18}O) concentrations, and found that 24 % of the 1192 mm annual precipitation exited the hillslope model domain as subsurface stormflow via preferential flow. Stumpp and Maloszweski (2010) used weekly ^{18}O samples in a lysimeter study to model the fraction of preferential flow in the lysimeter outflow for different cropping periods. Using a lumped parameter approach and HYDRUS 1-D, they found between 1.1 and 4.3 % preferential flow for the lumped parameter approach and 1.1 and 20.5 % for the HYDRUS 1-D approach, respectively. Kumar et al. (1997) found between 10 and 20 % preferential flow per year at a tile-drained field site where the fractions were higher during intense precipitation events. In a similar study, Stone and Wilson (2006) used differences in surface water chloride concentrations and tile-drain baseflow concentrations to separate tile-drain discharge into a matrix and preferential flow component. Preferential flow was in total 11 and 51 % for two events while it was 40 and 81 % during peak flow.

What is clear from all of this work is that role of preferential flow is more complex than simply the transport of event water through soils or hillslope. The key question is how preferential flow paths interact with their surroundings. This has been well studied at the soil-profile scale (e.g. Noguchi et al., 1999). Germann and Niggli (1998) showed in macroporous soils that the momentum of flow increased with depth, so that preferential flow can continue for a long time and over a long distance, once initiated. Nimmo (2012) summarized examples where preferential flow occurred with unsaturated soil matrix. Weiler and Naef (2003) studied the role of preferential flow during the infiltration process and the interaction between those preferential-flow paths and the soil matrix. By using a dye tracer and soil profiles they found that preferential flow was initiated at the soil surface or at partially saturated soil layers. Weiler and Flühler (2004) classified water flow through soils based on dye pattern, and could distinguish between different levels of macropore–matrix interaction. Königer et al. (2010) used deutereated water to investigate flow processes in the unsaturated zone during a sprinkling experiment. They collected soil samples 12 and 35 days after irrigation and found a distinct change of deuterium (^{2}H) background towards the concentration of applied water within one meter depth. This interaction plays a crucial role in the water transported via macropores, as macropore flow depends on soil matrix infiltration capacity, soil moisture, interaction between macropores and matrix, and connectivity of macropores (Tsuboyama et al., 1994; Sidle et al., 2000, 2001).

Here we build upon recent work to examine hillslope-scale macropore–matrix interactions. In particular, we build upon recent detailed hillslope investigations by Kienzler and Naef (2008), who used ^{222}Rn to distinguish between subsurface flow supplied directly from precipitation and water displaced from saturated parts of the soil profile. We use a controlled experiment at a tile-drained agricultural field site. We employ multiple tracers within a series of field-scale irrigation experiments to investigate flow processes through macropores, the interaction between macropores and the soil matrix, and the source of the discharging water at a tile-drained field site. Our tile-drained field site is effectively a hillslope-scale lysimeter (Richard and Steenhuis, 1988) that allows us to address the following questions regarding macropore flow of old water:

1. What are the dominant flow pathways through the soil?
2. What are the interactions between macropores and the soil matrix and their influence on the system response?
3. What is the source of the tile-drain water?
4. Where in the soil profile does the pre-event water originate?

2 Study site and methods

The Weiherbach Valley is a nested rural catchment of 3.6 km^2 (upper catchment) and 6.3 km^2 (total) size located in a loess area in southwestern Germany. The geology is dominated by Keuper sandstone, marl and mudstone (lower and middle Triassic) and a loess layer of up to 15 m thickness. The climate is semi-humid with an average annual precipitation of 750–800 mm, average annual runoff of 150 mm and annual potential evaporation of 775 mm. The average annual air temperature is 8.5 °C. About 95 % of the catchment area is used for agricultural purposes, 4 % is forested and 1 % is paved. Ploughing is usually to a depth of 25 cm in early spring or early autumn, but has been mainly replaced in recent years by minimum till practice (5–10 cm depth). Most of the Weiherbach hillslopes exhibit a typical loess catena

with moist but drained Colluvisols located at the hill foot and drier Calcaric Regosols or Luvisols located at the top and mid-slopes, inducing a typical distribution of preferential flow paths (Zehe and Flühler, 2001b). Earthworms such as Lumbricus terrestris L. play an important role in developing these vertical preferential flow paths, which play a dominant role in the Weiherbach catchment in water and solute transport as they may reach more than one meter depth (Zehe and Flühler, 2001a, b; Klaus and Zehe 2010, 2011). In addition epigeic earthworms populate the upper 30 cm of the soil.

2.1 Experimental site and determination of soil characteristics

The irrigation experiments were performed at a field site ($20 \times 20\,m^2$) with 10 m distance to the Weiherbach brook (49°08′08″ N, 8°44′42″ E), and with a gradient of $0.03\,m^1\,m^{-1}$. After being fallow land the site was reactivated for agricultural purposes 8 yr before the experiments. A single tile-drain tube is located about 1–1.2 m below the surface, embedded in a gravel layer, and entering the Weiherbach brook about 0.3 m above the baseflow water level. The soil is a Colluvisol with a strong gleyic horizon starting at a depth between 0.4 and 0.7 m below the surface.

Soil cores ($100\,cm^2$) were extracted from three different locations at five depths (between 0.075 m and 0.60 m, non-uniformly between the different locations) to measure soil hydraulic conductivity (constant and falling head method) and porosity. The soil hydraulic conductivity showed stratification with decreasing hydraulic conductivity, decreasing porosity, and increasing bulk density with depth. The hydraulic conductivities were $5.3 \times 10^{-8}\,m\,s^{-1}$, $1.8 \times 10^{-8}\,m\,s^{-1}$, and $1 \times 10^{-9}\,m\,s^{-1}$ at 0.5–0.6 m depth, and between $1 \times 10^{-4}\,m\,s^{-1}$ and $1 \times 10^{-6}\,m\,s^{-1}$ in the upper 0.1 m. The soil porosity decreased from approximately 0.5 to 0.4, and the bulk density increased from $1.3\,kg\,m^{-3}$ to $1.7\,kg\,m^{-3}$. The measured values are consistent with published soil data of Delbrück (1997) and Schäfer (1999). Soil tillage of the experimental field has been annual conventional ploughing to a depth of about 0.25–0.30 m. The experiments were performed before the annual soil tillage took place.

2.2 Experimental design of the study

Most experimental studies that perform irrigation experiments are singular events. The idea of this study was to perform a series of repeated irrigation experiments (three in total), together with an approach that combines hydrometric measurements with tracer observations. The series was performed with slightly different initial conditions between the experiments.

2.2.1 Experimental setup

The first experiment was performed on 16 September 2008, the second on the 15 September 2009, and the third three weeks later on the 5 October 2009. Meteorological conditions for the weeks before the experiments were logged at a nearby meteorological station. The irrigation was performed with a system of eight garden sprinklers (e.g. Wienhöfer et al., 2009). The irrigation amount was observed, and the duration and amount of the irrigation is summarized in Table 1. Soil moisture was observed during all experiments. The tile drain was sealed by a plastic board with a triangular notch (opening angle was 25°) and the water level was measured during the experiment by means of a pressure probe (PD-2, Sommer, Koblach, Austria) with a temporal resolution of 1 min and then a 10 min resolution after the experiments. Water levels were transformed into discharge using a rating curve that was determined by frequent discharge measurements with a bucket during the experiments. We estimate the accuracy at $0.02\,L\,s^{-1}$, which is determined by the accuracy of the pressure probe and the rating curve.

Bromide was applied as a tracer during the irrigation in the first two experiments. The isotopic signature (δ^2H and $\delta^{18}O$) of the irrigation water was sampled for all experiments. The background was sampled in the tile drain and the irrigation water. The tile-drain flow was sampled at variable intervals. We observed the isotopic signature of the soil water in the second experiment to determine the extent of the macropore–matrix interaction and the source of the tile-drain outflow. The isotopic composition of soil water was measured at three locations along a transect, from the near stream boundary of the field plot to the upper boundary. Sampling was performed with a hand auger to a depth of 0.6 m; the sampling holes were closed afterwards. Samples collected after the experiment were taken approximately 0.5 m away from the pre-experiment samples.

2.2.2 Pre-experiment condition

No continuous on-site measurement of soil moisture exists, thus we report the precipitation and potential evaporation (after Haude, 1955) for 45 days and 10 days before the experiment (Table 2). The 45 day period for the third experiment is given without the irrigation sum of the second experiment. The first experiment took place after a summer with more than three times the precipitation of the second experiment. The potential evaporation, on a 45 day basis, was lower for the first experiment.

Macropores generated by earthworms are the main factor of vertical preferential pathways in the Weiherbach catchment (Zehe and Flühler, 2001a, b) and were counted directly outside the boundary of the irrigation plot on two horizontal soil profiles at a depth of 0.10 m after the first two experiments (Table 3). This was done by excavating and cleaning the soil profiles. The pores were counted and their diameter measured; burrows or channels with a diameter below 2 mm were not included.

Table 1. Summary of irrigation for each experiment, duration (D), amount (A), and intensity (Int) for every irrigation block. Also the return period (based on 24 h) based on the empirical and a fitted cumulative distribution function. Standard deviation is given for the precipitation sums in brackets.

	Block 1			Block 2			Block 3			Total	Return Period
	D (min)	A (mm)	Int (mm h^{-1})	D (min)	A (mm)	Int (mm h^{-1})	D (min)	A (mm)	Int (mm h^{-1})	Sum (mm)	Days
Experiment 1	80	12.3 (8.7)	9.3	60	11.9 (9.7)	11.9	80	9.7 (5.4)	7.28	33.9 (22.2)	353–445
Experiment 2	35	5.3 (2.3)	9.1	90	17.6 (8.9)	11.7	90	18.2 (8.9)	12.1	41.1 (18.6)	667–850
Experiment 3	90	18.1 (9.9)	12.1	90	21.8 (11.6)	14.5	–	–	–	39.9 (18.9)	667–750

Table 2. Pre-experimental conditions.

	Date	45 day precipitation mm	10 day precipitation mm	45 day potential evaporation mm	10 day potential evaporation mm
Experiment 1	16 September 2008	137	10.9	102.8	15.3
Experiment 2	15 September 2009	43.3	9.2	146.2	24.1
Experiment 3	05 October 2009	30.1	0	109.2	19.5

2.2.3 Experiment details

First experiment

The irrigation rate was measured with 10 precipitation samplers, each with a support of 200 cm^2 and an opening located 0.30 m above ground. Irrigation occurred in three blocks: 60 min, 80 min, and 60 min. There were 30 min breaks between each block. A tracer solution (1500 L) containing 1600 g bromide was applied during the first irrigation block from 15 min to 35 min elapsed time. The irrigation water had a constant isotopic signature ($\delta^{18}O = -8.1$ ‰, $\delta^{2}H = -56.1$ ‰).

The day before the experiment, six plastic access tubes, with a diameter of 27 mm, were installed vertically into the soil via drilled access holes. The access tubes were installed without disturbing the surrounding soil matrix. These access tubes were used to measure soil moisture with a "Profile Probe – PR2" (Delta-T Devices, Burwell, UK) at six different depths (0.10, 0.20, 0.30, 0.40, 0.60, and 1 m) and at six locations (5, 10, and 15 m from the front end; 5 and 15 m from the left side). These measurements were performed before and after the irrigation, and in-between the irrigation blocks.

Background concentrations of bromide, ^{18}O, and ^{2}H were measured in both the tile drain and the irrigation water. In the beginning, the tile drain was sampled manually with a temporal resolution of five minutes, as Zehe and Flühler (2001a) reported a very fast first tracer breakthrough at a nearby field site. The sampling frequency was later reduced. In total, 51 water samples were collected during the experiment and the two hours following irrigation. The falling limb of the hydrograph was sampled every eight hours for five days by an automatic sampler (Teledyne Isco, Nebraska, USA). Six and seven days after the irrigation two additional samples were taken by hand.

Second experiment

Based on the results of the first experiment, measurements of the irrigation rate and soil moisture were improved. The irrigation rate was measured with 20 evenly distributed precipitation samplers, each with a support of 37.4 cm^2 and located approximately 0.05 m above ground. Irrigation occurred in three blocks (35 min, 90 min, and 90 min) with breaks of 22 min and 30 min in-between blocks. We applied 2400 g of bromide dissolved in 1500 L water with the first irrigation block (13 to 35 min). The irrigation water had a constant isotopic signature during the experiment ($\delta^{18}O = -8.35$ ‰, $\delta^{2}H = -56.0$ ‰).

To measure soil moisture continuously, six Theta Probes (Delta-T Devices, Burwell, UK) were installed in a vertical soil profile at the streamside boundary of the experimental plot at depths of 0.10 m, 0.30 m, and 0.50 m, with two at each depth. The moisture content was logged every five minutes with the DL6 (Delta-T Devices, Burwell, UK). Soil moisture was measured at 20 evenly distributed locations at the field site before and after the experiment, and in-between the irrigation blocks with a Theta Probe.

A total of 25 water samples were collected during the experiment at intervals of 15 min. The last two samples were collected at intervals of 30 min, and three additional samples were collected the day after the experiment.

Table 3. Number of worm burrows with specific diameters (d) per square meter, measured at two plots for the first two experiments in a depth of 10–15 cm.

Diameter	2–3 mm	3–5 mm	> 5 mm	Total
Plot 1, Experiment 1	68	20	0	88
Plot 2, Experiment 1	40	8	1	49
Plot 1, Experiment 2	65	21	2	88
Plot 2, Experiment 2	90	19	1	110

Third experiment

The irrigation rate was measured with the same method as the second experiment. Irrigation was performed in two 90-min blocks with a 30 min break in-between. No bromide was applied and the irrigation water had a constant isotopic composition ($\delta^{18}O = -8.31$ ‰, $\delta^{2}H = -56.1$ ‰). Unfortunately, wild boars destroyed the soil moisture equipment before this experiment, so only surface moisture was measured. Measurements were taken before and after the experiment, and in-between the irrigation blocks. A total of 21 samples were collected during the experiment at an interval of 15 min.

2.2.4 Determination of irrigation rate

Based on the 10 (1st experiment) and 20 (2nd and 3rd experiment) irrigation samplers, we evaluated the spatial correlation structure of the irrigation rates by calculating experimental variograms (Kitanidis, 1997) and fitting theoretical variogram functions. No correlation structure was revealed by this geostatistical analysis; therefore an average irrigation rate was determined using the mean value of all samplers (Table 1).

2.3 Chemical and isotope analytics

2.3.1 Water samples

Bromide and isotopes were measured directly in filtered (450 nm) water samples. Bromide concentrations were determined by anion chromatography (ICS-1000 Dionex). The detection limit is 0.1 mg L^{-1}.

For hydrogen isotope analysis ($^{2}H/^{1}H$), water samples were reduced to molecular hydrogen in a uranium reactor, and the gas was subsequently introduced into the inlet of an isotope ratio mass spectrometer (Delta-S, Finnigan MAT, Germany) where it was measured against a hydrogen monitoring gas. For oxygen isotope analysis ($^{18}O/^{16}O$) water samples were degassed and equilibrated with CO_2 of known isotopic composition. The CO_2 was subsequently introduced into the dual inlet of an isotope ratio mass spectrometer (Delta-S, Finnigan MAT, Germany) and measured again relative to a CO_2 monitoring gas. In both cases, calibration was accomplished with three in-house standards that were calibrated against the international reference materials VSMOW (Vienna Standard Mean Ocean Water), SLAP (Standard Light Antarctic Precipitation) and GISP (Greenland Ice Sheet Precipitation)(International Atomic Energy Agency, IAEA, Vienna). Isotope values $\delta^{2}H$ and $\delta^{18}O$ were expressed in parts per thousand (‰) as

$$\delta^{18}O \text{ or } \delta^{2}H = \left(\frac{R_{Sample}}{R_{St}} - 1 \right) \times 1000,$$

where R_{Sample} is the respective $^{2}H/^{1}H$, or $^{18}O/^{16}O$ ratio, and R_{St} the Vienna-Standard Mean Ocean Water (absolute VSMOW ratio is $^{2}H/^{1}H = 155.76 \pm 0.05 \times 10^{-6}$ and $^{18}O/^{16}O = 2005.2 \pm 0.45 \times 10^{-6}$). The $\delta^{2}H$ measurements of water samples have a precision of ±1 ‰, those of $\delta^{18}O$ have a precision of ±0.1 ‰.

2.3.2 Analysis of soil water isotopic composition

The isotopic composition of soil water was determined using cavity ring-down laser spectrometry of water vapor equilibrated with the liquid soil-water phase. Soil samples were sealed in two nested gas-tight bags and equilibrated in a dry nitrogen atmosphere for 24 h under controlled temperature (±0.1 °C) conditions until water-vapor phase equilibrium had been established. Based on Majoube (1971) the isotopic composition of soil water was derived from the isotopic composition of water vapor based on temperature dependent thermodynamic equilibrium fractionation. Allison et al. (1987) demonstrated that water-vapor saturation and isotope equilibrium in the unsaturated zone prevail even in dry desert soil. Hendry et al. (2008) used the same equilibration principle for wet clay soil, establishing water isotope profiles in deep clay. Based on parallel equilibration experiments of soil samples wetted with known liquid water isotope standards, the rapid establishment of water-vapor equilibration and of the isotope equilibration within 24 h could be confirmed. A mass balance of soil water compared to the total amount of vapor at saturation indicates that Rayleigh effects are far below the analytical precision of 0.15–0.25 ‰ for $\delta^{18}O$ and of 1.0–1.5 ‰ for $\delta^{2}H$ VSMOW, and do not affect the results significantly. Analysis was completed using Picarro cavity ring-down laser spectrometry (Picarro Inc., Santa Clara, California) (Iannone et al., 2010) for water isotopes based on principles of tunable diode laser spectrometry (Gianfrani et al., 2003; Kerstel and Gianfrani, 2008; Gupta et al., 2009).

2.4 Determination of event water proportion in tile drain hydrograph

We used the bromide tracer to determine the fraction of event (irrigation) water in tile-drain discharge. The use of stable isotopes is not feasible for hydrograph separation because the isotopic composition of the soil water is not uniform (see Sect. 3.1.2). The pre-event water component is the sum of activated soil water and baseflow (a spring connected to the

drain and shallow groundwater). The baseflow remains constant, thus all additional water is irrigation water and soil water. We determined the bromide concentration in the event water using a weighting procedure that accounted for the pulse application of bromide (e.g. Weiler et al., 1999). We calculated the event water concentrations for the hydrograph separations as a time variant value C_e(t) as follows:

$$C_e(t) = \frac{M_{in}(t) - M_{out}(t)}{P(t)}, \quad (1)$$

where t is the experimental time in minutes, $M_{in}(t)$ is the bromide mass (g) that was applied on the field plot until time t, $M_{out}(t)$ is the bromide mass (g) that has left the system via the tile drain until time t, and $P(t)$ is the total irrigation amount applied on the plot until time t (liters). The hydrograph separation was then performed following a mass balance approach (e.g. Sklash and Farvolden, 1979):

$$Q(t) = Q_e(t) + Q_p(t), \quad (2)$$

where $Q(t)$ is the tile-drain discharge at time t, $Q_e(t)$ is the amount of event water in the discharge at time t, and $Q_p(t)$ is the amount of pre-event water in the tile-drain discharge at time t.

$$C(t)Q(t) = C_e(t)Q_e(t) + C_pQ_p(t), \quad (3)$$

where $C(t)$ is the total bromide concentration ($g\,L^{-1}$) in the tile drain at time t, and C_p is the bromide concentration of the pre-event water, in this case a zero concentration.

In addition to instantaneous separation at the time of sampling, we calculated the total amount of event water for the first 500 min of each experiment. We did not apply bromide in the third experiment, so no hydrograph separation was performed.

2.5 Determination of macropore-matrix interaction with isotopic data

The measured isotopic composition of soil water from the second experiment was used with a compartmental mixing-cell model (Woolhiser et al., 1982; Campana and Simpson, 1984; Adar et al., 1988; Klaus et al., 2008) to evaluate mixing in the soil profile. We tested two conceptual interaction models (Fig. 1) and calculated the macropore–matrix interaction by mixing of event and pre-event water within soil compartments for the three sampled locations. The compartments were determined by the sampling depth of the soil water isotopes and represent a soil layer of undefined thickness at the sampling depths. The analysis is based on the following assumptions:

1. The measured pre-experiment soil water isotopic composition represents the average composition of the sampled soil matrix compartment.

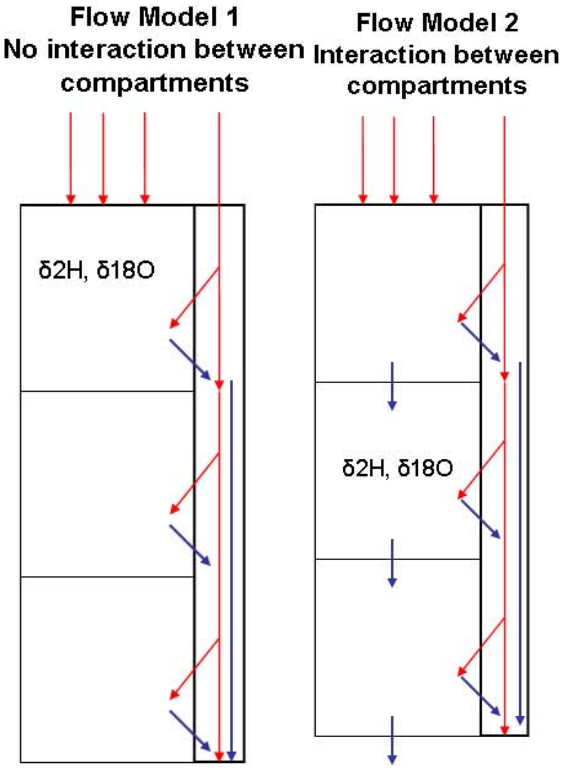

Fig. 1. Perceptual flow models for interaction of macropores and soil matrix compartments. Red arrows denote for the irrigation water, blue arrows denote for soil water. The boxes represent soil layers, while the continuous box represents a preferential flow path.

2. The measured post-experiment soil water isotopic composition represents the soil matrix isotopic composition. As the macropores started to empty after the irrigation stopped, at the time of sampling (90–120 min after the experiment), the macropores were empty.

The first model describes simple mixing of the pre-event matrix water with the irrigation water during the experiment, and the second model includes additional inflow from the soil compartment above. Calculations of the proportion between event and pre-event water were performed with ^{18}O and ^{2}H together. Here, the final water composition F is composed of event water E, pre-event water P, and water entering from the upstream cell U. Based on the following three equations:

$$x_1 + x_2 + x_3 = 1, \quad (4)$$

$$x_1C_{DE} + x_2C_{DU} + x_3C_{DP} = C_{DF}, \quad (5)$$

$$x_1C_{OE} + x_2C_{OU} + x_3C_{OP} = C_{OF}, \quad (6)$$

that denote for the water mass balance (Eq. 4) (and where x_1 is the fraction of irrigation water, x_2 the fraction of water from the above soil compartment, and x_3 the fraction of

water that was stored within a soil compartment before the experiment), the mass balance of ^{2}H (Eq. 5), and the mass balance of ^{18}O (Eq. 6), where C denotes the known isotopic composition while the subscripts "D" and "O" denote ^{2}H and ^{18}O, respectively, the following linear equation system can be derived:

$$\begin{pmatrix} 1 & 1 & 1 \\ C_{DE}/C_{DF} & C_{DU}/C_{DF} & C_{DP}/C_{DF} \\ C_{OE}/C_{OF} & C_{OU}/C_{OF} & C_{OP}/C_{OF} \end{pmatrix} \begin{pmatrix} x_1 \\ x_2 \\ x_3 \end{pmatrix} = \begin{pmatrix} 1 \\ 1 \\ 1 \end{pmatrix}. \quad (7)$$

Since x_1, x_2, and x_3 are constrained between 0 and 1 in Eq. (7), we applied linear programming to solve the mixing problem. The error was minimized by a least squares procedure.

3 Results

3.1 Hydrographs, tracer breakthrough curves and soil moisture

3.1.1 Experiment 1

Hydrograph behavior

Figure 2 (left column) presents the hydrograph and tracer data of the first experiment, while Table 1 summarizes the irrigation characteristics. Flow in the tile drain averaged 0.11 L s^{-1} for the 30 min period before the experiment. The first irrigation block caused no measurable increase in discharge. During the second irrigation block discharge increased abruptly. The hydrograph followed a double peak. The hydrograph peaked 8 min after the end of irrigation at 0.37 L s^{-1}. The total irrigation amount was 33.9 mm.

Tracer breakthrough curves

Isotopic background concentrations in the tile drain were −8.1 ‰ for δ^{18}O and −56.4 ‰ for δ^2H. The field site was irrigated with water of only slightly different isotopic composition (δ^{18}O = −8.35 ‰ and δ^2H = −58.5‰). Figure 2, left column, center row, presents the temporal variation of ^{18}O and ^{2}H in experiment 1. During the experiment both isotopes followed the shape of the hydrograph. The isotopic signature in the tile-drain water did not change in the direction of the irrigation water but instead became heavier than the background. The day after irrigation, δ^{18}O-values were back at the background level, while the δ^2H was slightly greater than the background.

Bromide exceeded the background concentration within 65 min after irrigation began (50 min after tracer application). Bromide concentrations are strongly correlated with the discharge, showing the same double peak. The coefficient of determination is $R^2 = 0.87$ on the rising limb of the hydrograph.

Soil moisture observations

Before the experiment, soil moisture showed drier conditions in the upper 0.30 m and higher moisture at 0.60 m and 1 m depths. Soil moisture at 0.10 m depth reached its maximum at four of six measuring locations after the first irrigation block, and remained constant throughout the day. At the two other soil moisture stations, maximum was reached after the second and third block, respectively. The soil moisture at 0.20 m depth at all locations increased slightly until 200 minutes elapsed and then stayed constant or decreased. The installation of the access tube, just the day before the experiment, limits the quality of the soil moisture data since the contact between the plastic tube and the soil was limited. The absolute measured moisture values are too high, considering that maximum measured porosity was at 54 %.

Main findings in the first experiment

An increase in tile-drain discharge did not begin directly after the start of the irrigation, however during the second irrigation block discharge was then strongly linked to the irrigation pattern. Some bromide was detected in the tile drain before the increase in discharge. At the moment when discharge clearly increased, bromide, ^{18}O, and ^{2}H concentrations increased. The change in isotopic composition indicates the contribution of soil water.

3.1.2 Experiment 2

Hydrograph behavior

The tile drain showed an average discharge of 0.10 L s^{-1} for the 30 min before the experiment (Fig. 2, center column). A significant increase in discharge began 105 min after onset of the experiment, leading to a double peak hydrograph. The main peak (0.31 L s^{-1}) occurred eight minutes after the end of irrigation. The total irrigation sum was 41.1 mm (Table 1).

Tracer breakthrough curves and soil water isotopes

Background δ^{18}O and δ^2H values in the tile drain were −8.0 ‰ and −57.5 ‰, respectively. The irrigation water had an isotopic composition of δ^{18}O = −8.3 ‰ and δ^2H = −56 ‰ . Again δ^{18}O and δ^2H followed the discharge dynamic (Fig. 2, center column, center plot), showing more enriched signatures with increasing discharge, peaking at −7.3 ‰ (^{18}O) and −50.4 ‰ (^{2}H). The fluctuations in ^{18}O were more erratic during the second experiment than during the first experiment and in general were more erratic than those of ^{2}H. The δ^{18}O values the day after the experiment were at background levels, as were those of deuterium.

The isotopic signature of the tile-drain discharge during irrigation showed heavier isotopic signatures than background

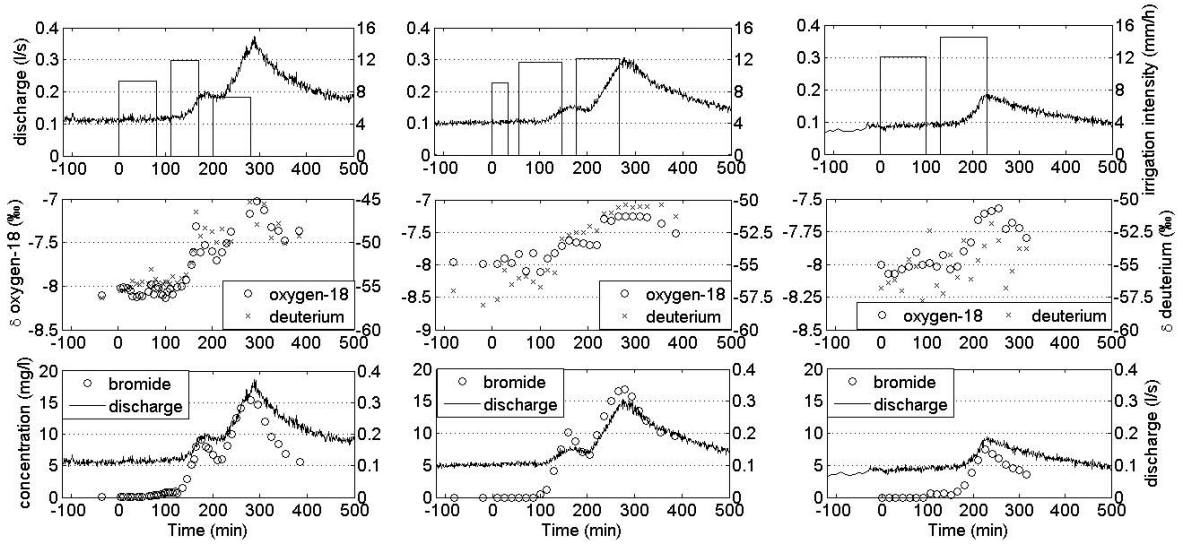

Fig. 2. Summary of the experiments, left column is experiment 1 (highest pre-experiment precipitation), center column experiment 2 (moderate pre-experiment precipitation), right column experiment 3 (lowest pre-experiment precipitation). Hydrographs, irrigation intensity, isotopic composition of tile-drain water, bromide and brilliant blue concentrations are plotted.

and irrigation signatures. The change observed in this experiment can clearly be associated with the observed isotopic signature of the soil water. The isotopic composition of soil water was measured before and after the experiment, this data is presented in Fig. 3 (the left column presents the ^{18}O values and the right column the deuterium values). The pre-experiment isotopic composition of soil water showed a decrease in the δ-values for both isotopes with increasing depth. This stratification is frequently observed in soil water studies (e.g. Barnes and Walker, 1989; Königer et al., 2010) and results from evaporation. After the irrigation experiment, the isotopic composition of soil water moved towards the composition of the irrigation water. The stratification with depth was conserved and no downward propagation of the isotope signal was observed.

The bromide concentrations exceeded the background value after 100 min, which occurred shortly before the increase in discharge. Bromide concentrations are strongly correlated with the hydrograph with a coefficient of determination of 0.9 at the rising limb. Bromide concentration peaked with 16.8 mg L^{-1}, and decreased after the end of the irrigation. The day after the experiment (not shown in Fig. 2), concentrations were still above background.

Soil moisture observation

Figure 4 summarizes the moisture dynamics during the experiment. The most rapid and strongest changes in soil moisture were measured at 0.10 m depth. Soil moisture at greater depths showed only small changes, remaining unsaturated throughout the experiment. The location of continuous soil-moisture observations were at the boundary of the irrigation area, where only minor ponding occurred. Surface soil moisture showed a uniform behavior. At the beginning of the experiment, surface soil moisture was measured between 18.5 % and 35 %, with an average of 28 % and a standard deviation of 4 %. Soil moisture increased, reaching average values of 36.7 % (standard deviation(SD) 4.5 %), 39.7 % (4 %) and 43.5 % (5.1 %) after the end of each irrigation block. Surface water ponding occurred in depressions at the end of the first irrigation block, and became widespread during the second irrigation block.

Main findings in the second experiment

The results of the first experiment were reproducible with the second. Tile-drain discharge started to increase during the second irrigation block. It seems that a certain amount of cumulated irrigation is needed to activate subsurface water flows. After activation, the irrigation pattern and the hydrograph are tightly linked. Isotope values increased until peak discharge was reached, becoming more distinct compared to tile-drain background and irrigation water. The data from the soil water isotopic composition showed the mobilization of soil water. Bromide concentrations slightly exceeded background values before discharge increased.

3.1.3 Experiment 3

Hydrograph behavior

Pre-experiment water level and discharge were lower than in the previous experiments (0.09 L s^{-1}). Approximately 180 min after the start of the irrigation, discharge increased

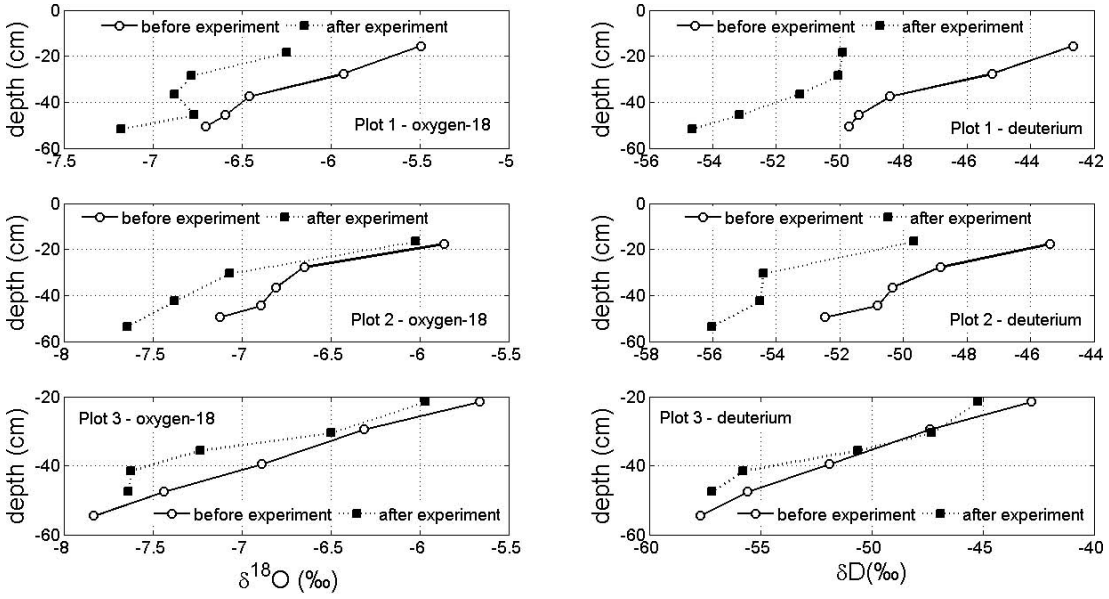

Fig. 3. Measured isotopic composition of soil water, before and after the second experiment at three sampling locations. Left column summarizes oxygen-18 (VSMOW in ‰) and the right column summarizes deuterium (VSMOW in ‰).

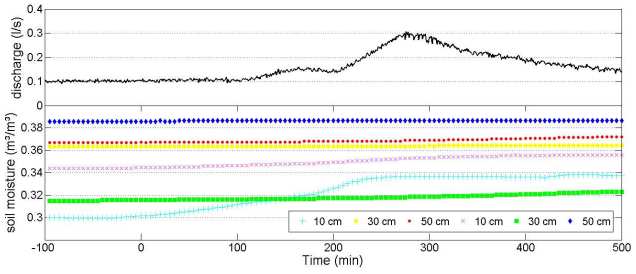

Fig. 4. Discharge and soil moisture dynamic during the second experiment, two theta probes for soil depths of 10 cm, 30 cm, and 50 cm, with a lateral distance of approximately 25 cm.

clearly and peaked with 0.19 L s^{-1} 230 min after the start of the experiment (Fig. 2, right column). After the peak, discharge decreased and reached the pre-event level about 300 min later. The total irrigation amount (Table 1) was 39.9 mm.

Tracer breakthrough curve

During the first 180 min of the experiment, the measured ^{18}O was not significantly different than the background value of −8 ‰. The ^{18}O value in irrigation water (−8.3 ‰) was more negative than the background value. With the increase in tile-drain discharge, δ^{18}O values increased markedly. The peak concentration of $\delta^{18}\mathrm{O} = -7.6$ ‰ was reached 255 min after the irrigation started. There was no clear pattern in the δ^{2}H values. The samples varied around a value of −55.0 ‰, with a maximum of −51.9 ‰ and a minimum of −57.8 ‰, and no clear temporal pattern.

Bromide was first detected (0.57 mg L^{-1}) 105 min after the irrigation began. Coincident with the increase of δ^{18}O values, bromide concentrations also clearly increased and peaked 225 min after the start of the experiment at a value of 7.48 mg L^{-1}. The contribution of bromide further proves a contribution from soil water.

Soil moisture observation

Surface soil moisture increased throughout the irrigation site. Ten out of 20 locations reached a maximum plateau value after the first irrigation block, indicating that saturation was reached. Average surface soil moisture was 26.8 % before the experiment with a standard deviation of 5.3 %, reached 42.8 % after the first irrigation block (SD = 2.7 %) and 44.9 % after the second block (SD = 3.3 %).

Main findings of the third experiment

Bromide was remobilized from the soil matrix during the experiment. This agrees with the observation of soil water activation from the water isotope data. However, the time of soil water activation is more clear for bromide than for the isotopes. Nevertheless, the soils within the system showed no contribution to tile-drain discharge at the beginning of the experiment.

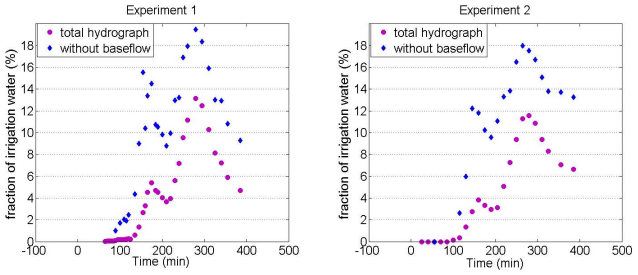

Fig. 5. Bromide based hydrograph separation of the first (left) and second (right) experiment. Shown is the proportion of irrigation water at the tile- drain discharge in the total measured discharge, and with baseflow subtracted.

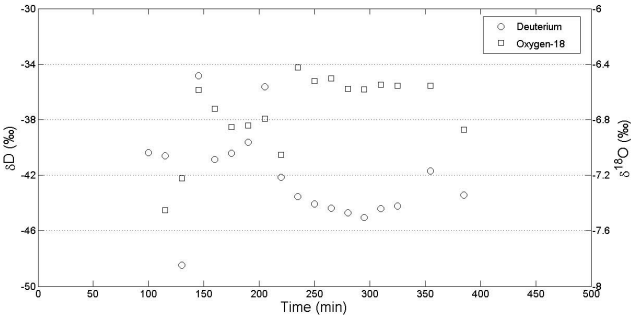

Fig. 6. The isotope values denote the calculated isotopic composition of the soil water contributing to the tile-drain discharge during the hydrograph of the second experiment.

3.2 Hydrograph separation to distinguish between event and pre-event water

Results of the hydrograph showed that the system is dominated by pre-event water (Fig. 5). Most of the mobilized water derived from the soil matrix. During the first experiment, the maximum proportion of event water was 13.2 % (19.5 %, when we only consider the activated water), corresponding to the highest bromide concentrations. The fraction of event water follows the double peak shape of discharge and bromide. In total, 5 % of the tile-drain discharge during the first 500 min of the experiment was event water and 12 % when we only considered the activated water.

Despite differences in the amounts of irrigation water and initial conditions, the event water fraction revealed the same pattern in the second experiment. The maximum proportions were slightly smaller, with 11.6 % (with baseflow) and 18 % (without baseflow). While the total proportion of event water was slightly higher at 6.2 % (13 % without baseflow). This latter observation resulted from the different shape of the declining hydrograph.

3.3 Compartmental modeling

Mixing between event and pre-event water was evaluated for every sampling location to account for the spatial variability derived from a variable preferential flow system within the experimental plot. Table 4 summarizes the results of the compartmental modeling. The results based on two end members (pre-event soil matrix water and irrigation water) indicate a clear interaction between soil matrix and the irrigation water throughout the depth of the profile. For example, at sampling location 1, the matrix water after the experiment consisted of 10.0 % to 34.1 % irrigation water, depending on the depth. The results for locations 2 and 3 are similar (Table 4). Using water from the overlying soil compartment as an additional end member led to somewhat different results. Location 3 showed contributions of water from overlying soil layers while this is not pronounced for locations 1 and 2.

With the applied linear programming, the sum of the individual errors of each mass balance equation (Eq. 7) is minimized. The mass balance error for each individual mass balance (water, ^{18}O and ^{2}H) showed a maximum deviation of -6.2 %. In total 71.6 % of the individual mass balance errors are below ± 2 %.

3.4 Determination of isotopic composition of soil water contributing to the hydrograph

The fractions of event water, soil water, and baseflow (assumed to be constant) are known, based on the hydrograph separation. The isotopic composition of the irrigation water and of baseflow is also known. The isotopic signature of the soil water contributing to the hydrograph may then be calculated using Eqs. (2) and (3) with three components. Figure 6 presents the calculated isotopic composition of contributing soil water. Combined with Fig. 3, we can estimate the soil depth that contributed water to the hydrograph. Results provided by ^{18}O and ^{2}H differ slightly in the estimated depths. During peak flow the calculated soil water signature of δ^{18}O values varies around -6.5 ‰, and the δ^{2}H values around -44 ‰ (Fig. 6). This corresponds to water from a soil depth of 0.2–0.4 m for ^{18}O and to a soil depth around 0.2 m for ^{2}H. These calculations are very sensitive to (a) measured discharge, (b) calculated fraction of event water, and (c) measured concentration, which can explain the discrepancy. For example, an assumed baseflow of 0.08 L s^{-1} compared to the measured 0.10 L s^{-1} would change the δ^{2}H values around peak flow from -46 ‰ to -47 ‰. Additionally, the spatial variation in isotopic composition of soil water can be higher than the observed variation within three profiles.

Table 4. Results of the compartmental-mixing modeling performed for every location, and for the two and three end-member modeling. Soil depth is the center depth of a soil compartment (cm), PESW is the proportion of pre-event soil matrix water in the soil compartment (%), IW is the proportion of irrigation water in the soil compartment (%), OC is the proportion of water from the overlying cell (%), Error WB the error in the water balance (%), Error ^{2}H is the error in the mass balance of deuterium (%), and Error ^{18}O is the error in the mass balance of oxygen-18 (%).

Compartment	Soil depth (cm)	PESW	IW	OC	Error WB	Error ^{2}H	Error ^{18}O
Location 1, two components							
1	−15.5	76.29	23.71	–	−2.10	6.17	−3.52
2	−27.5	65.94	34.06	–	−0.64	1.70	−1.02
3	−37.5	77.96	22.04	–	−0.82	1.87	−1.00
4	−45.5	90.05	9.95	–	−1.88	4.04	−1.93
5	−50.5	74.42	25.58	–	−1.77	3.99	−1.99
Location 1, three components							
2	−27.5	66.59	33.36	0.05	−0.79	1.70	−0.92
3	−37.5	77.45	22.54	0.01	−0.76	1.85	−1.08
4	−45.5	90.12	9.88	0.00	−1.89	4.04	−1.92
5	−50.5	0.01	29.89	70.10	−1.76	3.87	−1.89
Location 2, two components							
1	−17.5	89.17	10.83	–	−2.05	5.04	−2.63
2	−27.5	85.48	14.52	–	−1.89	4.85	−2.62
3	−36.5	72.76	27.24	–	−1.53	3.29	−1.61
4	−44.5	63.43	36.57	–	−1.24	2.59	−1.25
5	−49.5	67.85	32.15	–	−1.24	2.14	−0.84
Location 2, three components							
2	−27.5	85.56	14.44	0.00	−1.90	4.85	−2.61
3	−36.5	74.07	25.89	0.04	−1.66	3.30	−1.45
4	−44.5	63.27	36.72	0.00	−1.23	2.59	−1.27
5	−49.5	66.76	33.24	0.01	−1.16	2.15	−0.94
Location 3, two components							
1	−21.5	87.71	12.29	–	−0.43	1.28	−0.83
2	−29.5	94.26	5.74	–	0.54	−1.22	0.71
3	−39.5	59.34	40.66	–	−0.33	0.55	−0.21
4	−47.5	88.30	11.70	–	−1.30	1.43	−0.09
5	−54.5	100.00	0.00	–	0.18	2.02	−2.12
Location 3, three components							
2	−29.5	34.76	20.31	44.93	−0.01	−0.08	0.09
3	−39.5	34.52	48.65	16.83	−0.50	1.19	−0.65
4	−47.5	95.72	4.20	0.09	−1.63	1.18	0.51
5	−54.5	32.89	0.00	67.11	−1.81	2.56	−0.66

4 Discussion

4.1 The role of subsurface mixing and threshold behaviour

"Macropore flow of old water" is really a euphemism for a complex range of water mixing issues that occur from plot-scale vertical infiltration to lateral flow at the hillslope scale. Such subsurface mixing processes have frequently been observed in field studies (e.g. Buttle and Peters, 1997; Noguchi et al., 1999) and have a strong influence on the conceptualization of preferential flow systems across scales (e.g. Sidle et al., 2000, 2001). At our research site, earthworm-induced vertical preferential flow paths linked to the tile-drain system are the most important and connected fast-flow paths. Furthermore, our observed preferential flow paths are continuous to depths of one meter or more (as shown earlier at the

site by Zehe and Flühler, 2001a). Although surface ponding and continuous, deep, vertical, preferential flow paths were observed, our bromide-based hydrograph separation revealed that most of the tile-drain discharge was comprised of displaced soil water. This was consistent in the first two experiments regardless of the initial conditions and the irrigation characteristics.

Flow processes in the soil matrix, such as pressure waves (Torres et al., 1998; Williams et al., 2002) or translatory flow (Horton and Hawkins, 1965; Hewlett and Hibbert, 1967), have often been used to explain displacement and old water dominance of channel stormflow. Such processes would be expected to lead to a downward propagation of the isotope signal in the soil water through the profile. However, our measured isotope profile of soil water (Fig. 3) did not show any evidence of such downward propagation of the isotope signal. Rather this indicates mixing of irrigation water and the pre-event soil water throughout the depth of the profile. We attribute this mixing to the interaction of the preferential flow paths and the soil matrix. Our mixing-model results were consistent with this interpretation and past observational work (Flury, 1996; Zehe and Flühler, 2001a; Weiler and Naef, 2003; Van Schaik et al., 2008).

Closer examination of our isotope data from the tile drain and within the soil profile revealed that the soil was indeed not well mixed. Tile-drain water appeared to be sourced within the profile at a particular depth of 0.2–0.4 m (Fig. 6) during the main hydrograph peak. This suggests that a mixing layer exists within the upper soil, that, when saturated or near saturation, initiates preferential flow at a distinct soil depth (Steenhuis et al., 1994; Shalit and Steenhuis, 1996). At our site, epigeic earthworms live in the upper soil and appear to promote mixing in the surface soil. Figure 7 presents our simple, conceptual, vertical flow model consisting of two phases (before and after threshold initiation). Once the soil water capacity threshold (itself controlled by initial soil moisture and irrigation amount) was reached, soil water contributions were activated and entered the vertical preferential flow paths. Such a threshold behavior is similar to other recent threshold observations in hillslope-scale activation (Tromp-van Meerveld and McDonnell, 2006a, b; Zehe et al., 2007). Bromide was observed leaching into the tile-drain before this threshold was reached, indicating that some preferential flow paths are active prior to saturation. We hypothesize that after the threshold is reached, the vertical preferential flow paths were initiated by a mixture of irrigation water and old (stored) water from the upper soil mixing zone. Additionally, contributions of deeper soil layers could be initiated based on patches of local saturation. Isotope data from the earlier phase of the experiment suggest contributions from deeper soil water, which are not observable during high discharge in the tile drain.

Our work is consistent with tracer based findings of old water flow in preferential flow paths at the hillslope scale (e.g. McDonnell, 1990; Kienzler and Naef, 2008). But, what

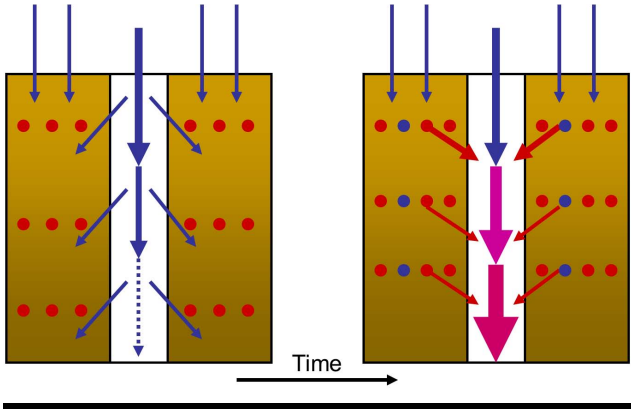

Fig. 7. Conceptual flow model of the field soil. Brown color indicates the soil matrix, the white box a preferential flow path. Red color indicates old water, blue color indicates new/irrigation water. Violet indicates mixed waters. At the beginning of the experiment (left) irrigation water infiltrates in the soil matrix at the surface and via macropores, only a small amount of irrigation water reaches the tile drain. With increasing storage in the system soil water enters the preferential flow paths and mixes there with irrigation water. Mostly old water reaches the tile drain.

is new with our work is our ability to specify where in the soil profile the old water comes from. In the experiments 1 and 2, the isotopic composition of the tile-drain flow was similar before and after the experiments (Fig. 8). During the event hydrograph, soil water contributions led to different signatures during the rising and falling limbs of the hydrograph. Figure 8 shows the temporal development of source regions and source fractions. At our site, old water delivery to the macropores is linked to the vertical orientation of the preferential flow paths and their direct link to the tile drain – all part of the overall hillslope, lateral, preferential flow structure. Elsewhere, we might imagine that hillslopes with a vertical and a lateral preferential flow system will have increased complexity in their mixing dynamics, especially if the macropores are short (Noguchi et al., 1999) or end without direct connectivity to the lateral flow path (McDonnell, 1990). Here the preferential flow paths are already initiated by a mixture of old and new water in a soil depth of 0.2–0.4 m, and are further fed by old water along their flow paths.

4.2 On the importance of our findings for catchment-scale hydrograph separation studies

Our work has important implications for isotope-based hydrograph separations at the catchment scale. Such hydrograph separations are based on the assumption that soil water does not contribute to the storm hydrograph or that its composition is similar to that of groundwater (Sklash and Farvolden, 1979). At this site we observed a mobilization of soil water and the additional activation of vadose zone water that invalidates the previous assumption (e.g. DeWalle et

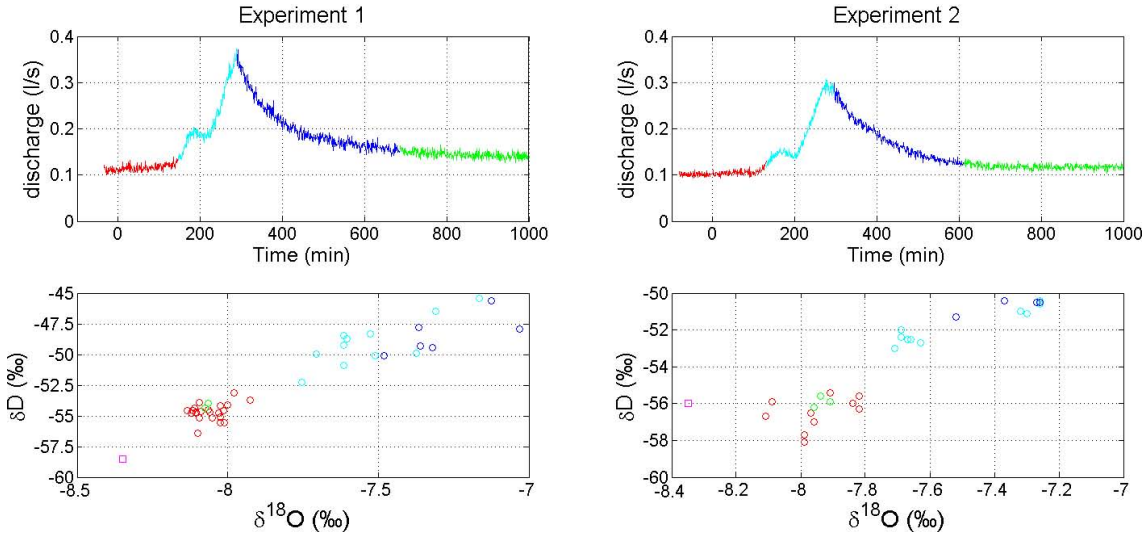

Fig. 8. Correlation between hydrograph phases and isotopic composition of tile-drain water. Left column are the results of the first experiment and the right column for the second experiment. Magenta denotes the isotopic composition of the irrigation water, light blue the isotopic composition of the rising hydrograph limb, dark blue the isotopic composition of the falling hydrograph limb, red the isotopic composition of baseflow conditions, and green the isotopic composition after the event.

al., 1988). There have been numerous studies that show two component source fractions exceeding 100 % (e.g. Swistock et al., 1989), and several studies have shown the importance of vadose zone contributions to storm runoff by sampling the soil water end-member and quantifying its effect on the hydrograph composition in the context of hydrograph separation (Kennedy et al., 1986; Swistock et al., 1989; Bazemore et al., 1994; Kendall et al., 2001). In theory, the use of a three-component hydrograph separation, accounting for soil water contributions, can help to overcome this (e.g. Ogunkoya and Jenkins, 1993).

Our work showed that a distinct layer of soil water, with a different isotopic signature than the deeper soil water, contributed water to the preferential flow paths. Such a selective contribution of one end-member can cause high uncertainty if the average isotopic composition of the soil water is used in the separation procedure. Thus the spatial variability of soil water must be considered on the catchment scale, both in depth and in areal extent. If hydrological connectivity increases during an event, a progressively greater soil volume contributes to subsurface runoff and catchment discharge. A variable source soil volume approach can help provide a framework for such a description of pre-event water at catchments (e.g. Harris et al., 1995). This is analogous to the variable source area concept used to describe the catchment runoff process (Hewlett and Hibbert, 1967; Dunne and Black, 1970).

5 Conclusions

We employed multiple tracers within a series of field scale irrigation experiments to investigate flow processes through a low-complexity macropore system, the interaction between macropores and the soil matrix, and the source of the discharged water at a tile-drained field site. We found that water transport through soil was governed by macropore flow and that macropore flow was itself a mixture of event and pre-event water. This pre-event water entered the preferential flow path during the initialization of the macropore flow based on mixing in the surface soil and contribution of saturated soil patches and their interaction with the preferential flow paths. The processes occurred independently of the initial conditions and the return period of the events. Although these processes will most likely not occur during low intensity precipitation events, and they will be different in other landscapes, they are characteristic of the investigated Weiherbach catchment during stormflow-initiating events. The combination of soil water isotope measurement, hydrograph separation based on applied bromide, and high frequency isotope sampling in the tile-drain outflow during three experiments let us identify the dominating processes at our field site and led to the following conclusions for this research site:

1. Preferential flow in the vertical macropores of anecic earthworms controls the flow to the tile-drain system.

2. Below a soil storage threshold, water from the preferential flow paths enters the soil matrix, while this process is reversed after the threshold is exceeded.

3. More than 80 % of the tile-drain discharge (above baseflow) is derived from the soil matrix, while less than 20 % is derived from the irrigation water.

4. The stable isotope data shows that this soil water is sourced from a depth of 0.2–0.4 m in the soil profile, consistent with the extent of a shallow network of earthworm channels promoting mixing.

Acknowledgements. We want to thank Markus Morgner, Juliane Palm, Peter Schwarz, Sibylle Steinbeiss, and Loes van Schaik for their support in the field. We thank Stephanie West for the support in the lab. We thank Petra Seibel and Harald Lowag for technical assistance with water isotope measurements, Doug Burns for comments on an earlier version of the manuscript, and Tina Garland for proof reading of the final manuscript. We also thank three anonymous reviewers for their comprehensive reviews and suggestions and Kevin Bishop for handling the manuscript as editor. Funding of this work by Deutsche Forschungsgemeinschaft (German Research Foundation) is gratefully acknowledged. (DFG Grant. ZE 533/5-1 and SSCHR 1000/3-1 "Linking spatial patterns of anecic earthworm populations, preferential flow pathways and agrochemical transport in rural catchments: an ecohydrological model approach"). We acknowledge support by Deutsche Forschungsgemeinschaft and Open Access Publishing Fund of Karlsruhe Institute of Technology.

Edited by: K. Bishop

References

Adar, E. M., Neuman, S. P., and Woolhiser, D. A.: Estimation of spatial recharge distribution using environmental isotopes and hydrochemical data, I. Mathematical model and application to synthetic data, J. Hydrol., 97, 251–277, 1988.

Allison, G. B., Colin-Kaczala, C., Filly, A., and Fontes, J. C.: Measurement of isotopic equilibrium between water, water vapour and soil CO_2 in arid zone soils, J. Hydrol., 95, 131–141, 1987.

Barnes, C. J. and Walker, G. R.: The distribution of deuterium and oxygen-18 during unsteady evaporation from a dry soil, J. Hydrol., 112, 55–67, 1989.

Bazemore, D. E., Eshleman, K. N., and Hollenbeck, K. J.: The role of soil water in stormflow generation in a forested headwater catchment: synthesis of natural tracer and hydrometric evidence, J. Hydrol., 162, 47–75, 1994.

Bishop, K., Seibert, J., Köhler, S., and Laudon, H.: Resolving the Double Paradox of rapidly mobilized old water with highly variable responses in runoff chemistry, Hydrol. Process., 18, 185–189, doi:10.1002/hyp.5209, 2004.

Blöschl, G. and Zehe, E.: On hydrological predictability, Hydrol. Process., 19, 3923–3929, 2005.

Buttle, J. M. and Peters, D. L.: Inferring hydrological processes in a temperate basin using isotopic and geochemical hydrograph separation: A re-evaluation, Hydrol. Process., 11, 557–573, 1997.

Campana, M. E. and Simpson, E. S.: Groundwater residence times and recharge rates using a discrete-state compartment model and ^{14}C data, J. Hydrol., 72, 171–185, 1984.

Delbrück, M.: Großflächiges Bromid-Tracerexperiment zur räumlichen und zeitlichen Variabilität des Wassertransports an einem Lößhang, Naturwissenschaftlich-Mathematische Gesamtfakultät, Ruprecht-Karls-University of Heidelberg, Heidelberg, Germany, 1997.

DeWalle, D. R., Swistock, B. R., and Sharpe, W. E.: Three-component tracer model for stormflow on a small Appalachian forested catchment, J. Hydrol., 104, 301–310, 1988.

Dunne, T. and Black, R.: Partial Area Contributions to Storm Runoff in a Small New England Watershed, Water Resour. Res., 6, 1296–1311, 1970.

Flury, M.: Experimental Evidence of Transport of Pesticides through Field Soils-a review, J. Environ. Qual., 25, 25–45, doi:10.2134/jeq1996.00472425002500010005x, 1996.

Flury, M., Leuenberger, J., Studer, B., and Flühler, H.: Transport of anions and herbicides in a loamy and a sandy field soil, Water Resour. Res., 31, 823–835, 1995.

Germann, P. and Niggli, T.: Dissipation of Momentum during flow in soils, Hydrolog. Sci. J., 43, 537–548, 1998.

Gianfrani, L., Gagliardi, G., van Burgel, M., and Kerstel, E.: Isotope analysis of water by means of near infrared dual-wavelength diode laser spectroscopy, Opt. Express, 11, 1566–1576, 2003.

Gupta, P., Noone, D., Galewsky, J., Sweeney, C., and Vaughn, B. H.: A new laser-based, field-deployable analyzer for laboratory-class stable isotope measurements in water, Geochima. Cosmochim. Ac., 73, A480–A480, 2009.

Harris, D. M., McDonnell, J. J., and Rodhe, A.: Hydrograph Separation Using Continuous Open System Isotope Mixing, Water Resour. Res., 31, 157–171, doi:10.1029/94wr01966, 1995.

Haude, W.: Zur Bestimmung der Verdunstung auf möglichst einfache Weise. – Mitt. Dt. Wetterd. 2 (11), Bad Kissingen (Dt. Wetterdienst), 1955.

Hendry, M. J., Wassenaar, L. I., and Lis, G. P.: Stable isotope composition of gaseous and dissolved oxygen in the subsurface, Geochim. Cosmochim. A., 72, A367–A367, 2008.

Hewlett, J. D. and Hibbert, A. R.: Factors affecting the response of small watersheds to precipitation in humid areas, in: Forest Hydrology, edited by: Sopper, W. E. and Lull, H. W., Pergamon Press, New York, 275–290, 1967.

Horton, J. H. and Hawkins, R. H.: Flow path of rain from the soil surface to the water table, Soil Sci., 100, 377–383, 1965.

Iannone, R. Q., Romanini, D., Cattani, O., Meijer, H. A. J., and Kerstel, E. R. T.: Water isotope ratio (delta H-2 and delta O-18) measurements in atmospheric moisture using an optical feedback cavity enhanced absorption laser spectrometer, J. Geophys. Res., 115, D10111, doi:10.1029/2009jd012895, 2010.

Jarvis, N. J.: A review of non-equilibrium water flow and solute transport in soil macropores: principles, controlling factors and consequences for water quality, Euro. J. Soil Sci., 58, 523–546, doi:10.1111/j.1365-2389.2007.00915.x, 2007.

Kendall, C., McDonnell, J. J., and Gu, W.: A look inside "black box" hydrograph separation models: a study at the Hydrohill catchment, Hydrol. Proc., 15, 1877–1902, doi:10.1002/hyp.245, 2001.

Kennedy, V. C., Kendall, C., Zellweger, G. W., Wyerman, T. A., and Avanzino, R. J.: Determination of the components of stormflow using water chemistry and environmental isotopes, Mattole River basin, California, J. Hydrol., 84, 107–140, 1986.

Kerstel, E. and Gianfrani, L.: Advances in laser-based isotope ratio measurements: selected applications, Appl. Phys. B-Lasers O., 92, 439–449, doi:10.1007/s00340-008-3128-x, 2008.

Kienzler, P. M. and Naef, F.: Subsurface storm flow formation at different hillslopes and implications for the "old water paradox", Hydrol. Process., 22, 104–116, doi:10.1002/hyp.6687, 2008.

Kirchner, J. W.: A double paradox in catchment hydrology and geochemistry, Hydrol. Process., 17, 871–874, doi:10.1002/hyp.5108, 2003.

Kitanidis, P. K.: Introduction to Geostatistics: Applications in Hydrogeology, Cambridge University Press, Cambridge, UK, 271 pp., 1997.

Klaus, J. and Zehe, E.: Modelling rapid flow response of a tile-drained field site using a 2D physically based model: assessment of "equifinal" model setups, Hydrol. Process., 24, 1595–1609, doi:10.1002/hyp.7687, 2010.

Klaus, J. and Zehe, E.: A novel explicit approach to model bromide and pesticide transport in connected soil structures, Hydrol. Earth Syst. Sci., 15, 2127–2144, doi:10.5194/hess-15-2127-2011, 2011.

Klaus, J., Külls, C., and Dahan, O.: Evaluating the recharge mechanism of the Lower Kuiseb Dune area using mixing cell modeling and residence time data, J. Hydrol., 358, 304–316, 2008.

Königer, P., Leibundgut, C., Link, T., and Marshall, J. D.: Stable isotopes applied as water tracers in column and field studies, Org. Geochem., 41, 31–40, 2010.

Kumar, A., Kanwar, R. S., and Hallberg, G. R.: Separating preferential and matrix flows using subsurface tile flow data, J. Environ Sci. Heal. A, 32, 1711–1729, 1997.

Leaney, F. W., Smettem, K. R. J., and Chittleborough, D. J.: Estimating the contribution of preferential flow to subsurface runoff from a hillslope using deuterium and chloride, J. Hydrol., 147, 83–103, 1993.

Majoube, M.: Fractionnement en oxygène-18 et en deuterium entre l'eau et sa vapour, J. Chim. Phys., 197, 1423–1436, 1971.

McDonnell, J. J.: A rationale for old water Discharge Through Macropores in a Steep, Humid Catchment, Water Resour. Res., 26, 2821–2832, 1990.

Mosley, M. P.: Streamflow generation in a forested watershed, New Zealand, Water Resour. Res., 15, 795–806, doi:10.1029/WR015i004p00795, 1979.

Nimmo, J. R.: Preferential flow occurs in unsaturated conditions, Hydrol. Process., 26, 786–789, doi:10.1002/hyp.8380, 2012.

Noguchi, S., Tsuboyama, Y., Sidle, R. C., and Hosoda, I.: Morphological Characteristics Of Macropores And The Distribution Of Preferential Flow Pathways In A Forested Slope Segment, Soil Sci. Soc. Am. J., 63, 1413–1423, doi:10.2136/sssaj1999.6351413x, 1999.

Ogunkoya, O. O. and Jenkins, A.: Analysis of storm hydrograph and flow pathways using a three-component hydrograph separation model, J. Hydrol., 142, 71–88, 1993.

Richard, T. L. and Steenhuis, T. S.: Tile drain sampling of preferential flow on a field scale, J. Contam. Hydrol., 3, 307–325, 1988.

Schäfer, D.: Bodenhydraulische Eigenschaften eines Kleineinzugsgebiets – Vergleich und Bewertung unterschiedlicher Verfahren, University of Karlsruhe, Karlsruhe, Germany, 1999.

Shalit, G. and Steenhuis, T.: A simple mixing layer model predicting solute flow to drainage lines under preferential flow, J. Hydrol., 183, 139–149, doi:10.1016/s0022-1694(96)80038-2, 1996.

Sidle, R. C., Kardos, L. T., and van Genuchten, M. T.: Heavy Metals Transport Model In A Sludge-treated Soil, J. Environ. Qual., 6, 438–443, doi:10.2134/jeq1977.00472425000600040023x, 1977.

Sidle, R. C., Tsuboyama, Y., Noguchi, S., Hosoda, I., Fujieda, M., and Shimizu, T.: Stormflow generation in steep forested headwaters: a linked hydrogeomorphic paradigm, Hydrol. Process., 14, 369–385, doi:10.1002/(sici)1099-1085(20000228)14:3<369::aid-hyp943>3.0.co;2-p, 2000.

Sidle, R. C., Noguchi, S., Tsuboyama, Y., and Laursen, K.: A conceptual model of preferential flow systems in forested hillslopes: evidence of self-organization, Hydrol. Process., 15, 1675–1692, doi:10.1002/hyp.233, 2001.

Šimůnek, J., Jarvis, N. J., Genuchten, M. T. v., and Gaerdenaes, A.: Review and comparison of models for describing non-equilibrium and preferential flow and transport in the vadose zone, J. Hydrol., 272, 14–35, 2003.

Sklash, M. G. and Farvolden, R. N.: The role of groundwater in storm runoff, J. Hydrol., 43, 45–65, 1979.

Smettem, K. R. J., Chittleborough, D. J., Richards, B. G., and Leaney, F. W.: The influence of macropores on runoff generation from a hillslope soil with a contrasting textural class, J. Hydrol., 122, 235–251, 1991.

Steenhuis, T. S., Boll, J., Shalit, G., Selker, J. S., and Merwin, I. A.: A Simple Equation For Predicting Preferential Flow Solute Concentrations, J. Environ. Qual., 23, 1058–1064, doi:10.2134/jeq1994.00472425002300050030x, 1994.

Stone, W. W. and Wilson, J. T.: Preferential Flow Estimates to an Agricultural Tile Drain with Implications for Glyphosate Transport, J. Environ. Qual., 35, 1825–1835, doi:10.2134/jeq2006.0068, 2006.

Stumpp, C. and Maloszewski, P.: Quantification of preferential flow and flow heterogeneities in an unsaturated soil planted with different crops using the environmental isotope δ^{18}O, J. Hydrol., 394, 407–415, 2010.

Swistock, B., DeWalle, D., and Sharpe, W.: Sources of Acidic Storm Flow in an Appalachian Headwater Stream, Water Resour. Res., 25, 2139–2147, 1989.

Torres, R., Dietrich, W. E., Montgomery, D. R., Anderson, S. P., and Loague, K.: Unsaturated zone processes and the hydrologic response of a steep, unchanneled catchment, Water Resour. Res., 34, 1865–1879, doi:10.1029/98wr01140, 1998.

Tromp-van Meerveld, H. J. and McDonnell, J. J.: Threshold relations in subsurface stormflow: 1. A 147-storm analysis of the Panola hillslope, Water Resour. Res., 42, W02410, doi:10.1029/2004wr003778, 2006a.

Tromp-van Meerveld, H. J. and McDonnell, J. J.: Threshold relations in subsurface stormflow: 2. The fill and spill hypothesis, Water Resour. Res., 42, W02411, doi:10.1029/2004wr003800, 2006b.

Tsuboyama, Y., Sidle, R. C., Noguchi, S., and Hosoda, I.: Flow and solute transport through the soil matrix and macropores of a hillslope segment, Water Resour. Res., 30, 879–890, doi:10.1029/93wr03245, 1994.

Tsukamoto, Y. and Ohta, T.: Runoff process on a steep forested slope, J. Hydrol., 102, 165–178, doi:10.1016/0022-1694(88)90096-0, 1988.

Uchida, T., Kosugi, K., and Mizuyama, T.: Runoff characteristics of pipeflow and effects of pipeflow on rainfall-runoff phenomena in a mountainous watershed, J. Hydrol., 222, 18–36,

doi:10.1016/s0022-1694(99)00090-6, 1999.

Van Schaik, N. L. M. B., Schnabel, S., and Jetten, V. G.: The influence of preferential flow on hillslope hydrology in a semi-arid watershed (in the Spanish Dehesas), Hydrol. Process., 22, 3844–3855, doi:10.1002/hyp.6998, 2008.

Vogel, T., Sanda, M., Dusek, J., Dohnal, M., and Votrubova, J.: Using Oxygen-18 to Study the Role of Preferential Flow in the Formation of Hillslope Runoff, Vadose Zone J., 9, 252–259, doi:10.2136/vzj2009.0066, 2008.

Weiler, M. and Flühler, H.: Inferring flow types from dye patterns in macroporous soils, Geoderma, 120, 137–153, 2004.

Weiler, M. and Naef, F.: An experimental tracer study of the role of macropores in infiltration in grassland soils, Hydrol. Process., 17, 477–493, 2003.

Weiler, M., Scherrer, S., Naef, F., and Burlando, P.: Hydrograph separation of runoff components based on measuring hydraulic state variables, tracer experiments and weighting methods, IAHS Publications, 258, 249–255, 1999.

Wienhöfer, J., Germer, K., Lindenmaier, F., Färber, A., and Zehe, E.: Applied tracers for the observation of subsurface stormflow at the hillslope scale, Hydrol. Earth Syst. Sci., 13, 1145–1161, 10, http://www.hydrol-earth-syst-sci.net/13/1145/10/.5194/hess-13-1145-2009, 2009.

Williams, A. G., Dowd, J. F., and Meyles, E. W.: A new interpretation of kinematic stormflow generation, Hydrol. Process., 16, 2791–2803, doi:10.1002/hyp.1071, 2002.

Woolhiser, D. A., Gardner, H. R., and Olsen, S. R.: Estimation of multiple inflows to a stream reach using water chemistry data, Trans. A.S.A.E., 25, 616–626, 1982.

Zehe, E. and Flühler, H.: Preferential transport of isoproturon at a plot scale and a field scale tile-drained site, J. Hydrol., 247, 100–115, 2001a.

Zehe, E. and Flühler, H.: Slope scale variation of flow patterns in soil profiles, J. Hydrol., 247, 116–132, 2001b.

Zehe, E., Elsenbeer, H., Lindenmaier, F., Schulz, K., and Blöschl, G.: Patterns of predictability in hydrological threshold systems, Water Resour. Res., 43, W07434, doi:10.1029/2006wr005589, 2007.